TE Mode Excitation on Dielectric Loaded Parallel Plane and Trough Waveguides*

M. COHN†, MEMBER, IRE, E. S. CASSEDY‡, MEMBER, IRE, AND M. A. KOTT‖, MEMBER, IRE

Summary—A theoretical and experimental study of the launching of TE surface wave modes on dielectric loaded parallel plane and trough waveguides has been performed. The source is a linear transverse current filament perpendicular to and extending across the space between the parallel side walls. Families of curves are presented, which show the bidirectional launching efficiencies for the dominant TE modes of these two transmission lines as a function of dielectric constant, dielectric slab thickness, and current filament location. Measured bidirectional efficiencies are compared to the theoretically predicted values. Measured unidirectional launching efficiencies as high as 97 per cent were obtained for the case where a short circuit is located on one side of the current filament.

Introduction

THE FIELDS produced by a time varying current filament 1) embedded in an infinite dielectric slab of finite thickness, and 2) above and parallel to an infinite dielectric coated conducting plane have been analyzed respectively by Whitmer[1] and Tai.[2] The purpose of this extension of the works of Whitmer and Tai is to investigate the efficiency with which particular surface wave modes can be launched on these structures.

In the mathematical formulation of these problems,[1,2] physically unrealizable geometries and excitation conditions are assumed. The method of excitation is unrealizable since the current filament is assumed to be infinite in length and independent of the coordinate in the direction of current flow. If two parallel conducting planes, spaced a finite distance apart, are located on the above structures so as to be perpendicular to the current filaments, then the physically realizable dielectric loaded parallel plane[3,4] and through waveguides result. The fields which existed on the original unrealizable structures are undisturbed by the addition of the two parallel conducting planes, but the total power emanating from the unit current filament is now finite. The current filament can be energized from a coaxial line feeding through one of the side conducting walls, with only the center conductor crossing the lines and contacting the opposite wall. The variation of the current strength in the direction of its length can be made arbitrarily small by making the distance between the two parallel planes of the parallel plane (or trough) waveguide sufficiently small compared to the free space wavelength. It is thus possible to approximate closely the theoretically assumed conditions on practical transmission lines capable of supporting surface wave propagation. The existence of these surface wave structures provides the motivation for investigating efficient launching methods.

TE_{20} Mode Excitation and Dielectric Loaded Trough Waveguide

An analysis of the fields produced by a periodic time varying current filament above and parallel to a dielectric coated conducting plane has been performed by Tai.[2] Although Tai's analysis takes account of the existence of surface wave modes, his paper is primarily concerned with the effect on the radiation pattern caused by the introduction of the dielectric coating on the ground plane.

Tai has solved the inhomogeneous wave equation in the space shown in Fig. 1(a) to determine the electric field in region 2 (E_{y2}) created by the filamentary unit current element located along the line $x=d$, $z=0$. This method of excitation is unrealizable since the current is assumed to be independent of y and infinite in extent in the y-direction. The only field components that can exist, therefore, are E_y, H_x, and H_z. These field components will also be independent of y. If conducting planes are placed at $y=0$ and $y=b$, the above fields are undisturbed, and the physically realizable trough line configuration[3,4] of Fig. 1(b) results.

Tai has shown that the electric field in the region above the current filament ($x>d$) is given by

$$E_{y2}(x, z) = \frac{j\omega\mu_0}{2\pi}\int_{-\infty}^{\infty} \frac{k_1 \sinh k_2(d-a) + k_2 \tanh k_1 a \cosh k_2(d-a)}{k_2(k_1 + k_2 \tanh k_1 a)} e^{k_2(a-x)} e^{j\beta z} d\beta, \quad (1)$$

* Received by the PGMTT, May 16, 1960; revised manuscript received July 6, 1960. Research supported by the U. S. Air Force, through WWRNGW of the Wright Air Dev. Div. of the Air Res. and Dev. Command.

† Electronic Communications, Inc., Timonium, Md.
‡ Microwave Res. Inst., Polytechnic Inst. of Brooklyn, Brooklyn, N. Y.
‖ Radiation Lab., The Johns Hopkins University, Baltimore, Md.

[1] R. M. Whitmer, "Fields in nonmetallic waveguides," PROC. IRE, vol. 36, pp. 1105–1109; September, 1948.

[2] C. T. Tai, "The effect of a grounded slab on the radiation from a line source," *J. Appl. Phys.*, vol. 22, pp. 405–414; April, 1951.

[3] M. Cohn, "Propagation in a dielectric-loaded parallel plane waveguide," IRE TRANS. ON MICROWAVE THEORY AND TECHNIQUES, vol. MTT-7, pp. 202–208; April, 1959.

[4] M. Cohn, "TE modes of the dielectric loaded trough line," IRE TRANS. ON MICROWAVE THEORY AND TECHNIQUES, vol. MTT-8, pp. 449–454; July, 1960.

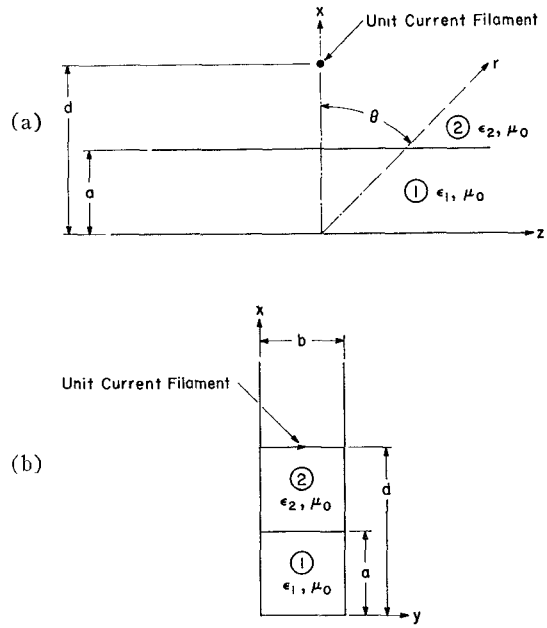

Fig. 1—(a) Dielectric coated conducting plane excited by an infinitely long unit current filament. (b) Dielectric loaded trough line excited by a unit current filament.

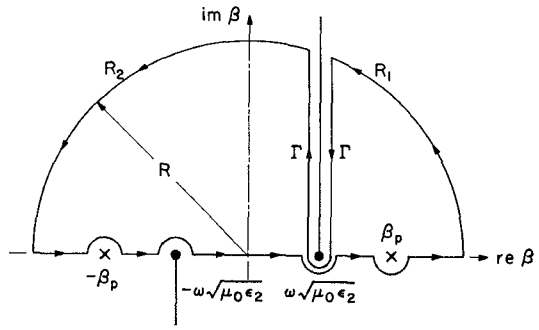

Fig. 2—Contour of integration in the β plane.

where k_1 and k_2 are the x-direction wave numbers of regions 1 and 2, which are related to the propagation constant (β), angular frequency (ω), permeability (μ_0) and permittivity (ϵ_1 or ϵ_2) by the following equations:

$$k_1^2 = \beta^2 - \omega^2\mu_0\epsilon_1, \tag{2}$$

$$k_2^2 = \beta^2 - \omega^2\mu_0\epsilon_2. \tag{3}$$

The real integral (1) is evaluated by considering it to be a contour integral in the complex β plane and applying the Cauchy Residue Theorem. The integrand of (1) is multiple valued at $k_1 = 0$ and $k_2 = 0$, but is an even function of k_1, and hence the only branch points occur at

$$\beta_b = \pm\,\omega\sqrt{\mu_0\epsilon_2}, \qquad (k_2 = 0).$$

The integrand of (1) has poles at $\pm\beta_p$ determined by

$$k_{1p} + k_{2p}\tanh k_{1p}a = 0, \tag{4}$$

where k_{1p} and k_{2p} are the transverse wave numbers k_1 and k_2 at the poles of (1). A path of integration in the complex β-plane which assures convergence of the integral is shown in Fig. 2. In the limit, as $R \to \infty$, the contributions to the integral from the circular arcs R_1 and R_2 approach zero. The integral (1) is therefore equal to the integral along the branch cut (Γ) plus the residue due to the pole at β_p. Prior to evaluating the branch cut contribution, the path of integration is deformed from Γ to a new path of steepest descent, which passes through the saddle point of the integrand. The coordinates are transformed to the cylindrical coordinate system shown in Fig. 1, following the method of Tai[2] but using a different coordinate system. Upon performing the saddle point integration, which is valid for large r, the following formula is found for the branch cut contribution to the electric field.

$$E_y^R \cong j\sqrt{\frac{\omega\mu_0}{2\pi}}\left(\frac{\mu_0}{\epsilon_0}\right)^{1/4} F(\theta)\,\frac{e^{j\beta_b r}}{\sqrt{r}} \tag{5}$$

where:

$$F(\theta) = \frac{\sqrt{K_1 - \sin^2\theta}\,\sin\left[\pi\left(\frac{2a}{\lambda_0}\right)\left(\frac{d}{a} - 1\right)\cos\theta\right]}{\left\{\sqrt{K_1 - \sin^2\theta} - j\cos\theta\tan\left[\pi\left(\frac{2a}{\lambda_0}\right)\sqrt{K_1 - \sin^2\theta}\right]\right\} e^{j\pi(2a/\lambda_0)\cos^2\theta}}$$

$$+ \frac{\cos\theta\tan\left[\left(\frac{2a}{\lambda_0}\right)\sqrt{K_1 - \sin^2\theta}\right]\cos\left[\pi\left(\frac{2a}{\lambda_0}\right)\left(\frac{d}{a} - 1\right)\cos\theta\right]}{\left\{\sqrt{K_1 - \sin^2\theta} - j\cos\theta\tan\left[\pi\left(\frac{2a}{\lambda_0}\right)\sqrt{K_1 - \sin^2\theta}\right]\right\} e^{j\pi(2a/\lambda_0)\cos^2\theta}} \tag{6}$$

$$\epsilon_2 = \epsilon_0, \qquad \epsilon_1 = K_1\epsilon_0, \qquad \beta_b = \omega\sqrt{\mu_0\epsilon_0} = \frac{2\pi}{\lambda_0}.$$

Eq. (5) is recognized as the electric field of a radially propagating cylindrical wave. Eq. (6) is the field intensity radiation pattern of this wave. In the degenerate case, when $a=0$, the radiation pattern reduces to the well known solution for a current filament above a ground plane.

The evaluation of the pole residue contribution to the total field requires some interpretation. If the homogeneous wave equation for TE modes on the source free trough line is solved, one obtains (4) as the necessary condition to satisfy the boundary conditions at the dielectric-air interface. Furthermore, when one evaluates the contour integral (1), the residue contributions from the poles are in the following form:

$$F(d, a, \lambda_0)e^{k_{2p}(a-x)}e^{j\beta_p z}.$$

It has been previously shown[3,4] that the above solutions represent modal solutions, or surface waves propagating in the z-direction. β_p must be real for a dissipationless structure. In order to satisfy the radiation condition, k_{2p} must be real and positive, which requires that k_{1p} be pure imaginary and restricted to certain intervals. Let $k_{1p}=jk_{1o}$ and $k_{2p}=k_{2o}$, where k_{1o} and k_{2o} are the symbols used for the transverse wave numbers describing the modal solutions. The subscripts "e" and "o" are used to denote respectively the modes having even and odd symmetry which can exist on the dielectric loaded parallel plane guide (only the odd modes can exist on the dielectric loaded trough line). By making use of (2), (3), and (4) and the fact that $k_{1p}=jk_{1o}$, the following result is obtained

$$\pi^2\left(\frac{2a}{\lambda_0}\right)^2(K_1-1)=\left[\frac{k_{1o}a}{\sin k_{1o}a}\right]^2. \tag{7}$$

Solutions of (7) which yield the characteristics of the TE_{mo} modes on the trough line are available.[3,4] The even symmetry modes correspond to m being an odd integer and vice versa. In order for the TE_{mo} mode to propagate, the following inequality must be satisfied:

$$\frac{2a}{\lambda_0}>\frac{m-1}{2\sqrt{K_1-1}}. \tag{8}$$

In the remainder of this analysis, it is assumed that only the pole corresponding to the TE_{20} mode (dominant mode of the trough line) exists. Therefore, the analysis is valid only for the following interval:

$$\frac{1}{2\sqrt{K_1-1}}<\frac{2a}{\lambda_0}<\frac{3}{2\sqrt{K_1-1}}.$$

When the pole residue is evaluated, the following expression for the electric field of the TE_{20} mode in region 2 is obtained:

$$E_{y2}^{s}(x,z)=\omega\mu_0\frac{(k_{10}a)\sin^2 k_{10}a}{(\beta_p a)(\tan k_{10}a-k_{10}a)}e^{-k_{20}(d-2a+x)+j\beta_p z}, \tag{9}$$

where

$$\beta_p^2=\omega^2\mu_0\epsilon_0K_1-k_{10}^2=\omega^2\mu_0\epsilon_0+k_{20}^2$$

and

$$\frac{\pi}{2}<k_{10}a<\pi.$$

By the use of (9) and the required boundary conditions at the dielectric-air interface, it is a routine matter to determine the other field components of the TE_{20} mode in regions 1 and 2. The total surface wave power flowing in the positive z-direction (P_z) can then be calculated, and when the power has been normalized with respect to the trough line width (b) and free space wavelength (λ_0), the following result is obtained:

$$\frac{P_z\lambda_0}{b}=60\pi^2\frac{(k_{10}a)^2\sin^2 k_{10}a}{\sqrt{\pi^2\left(\frac{2a}{\lambda_0}\right)^2K_1-(k_{10}a)^2}(k_{10}a-\tan k_{10}a)}\cdot e^{-2k_{20}a(d/a-1)}. \tag{10}$$

The values of k_{10} and k_{20} to be used in (10) may be obtained from the previous results of Cohn.[4]

By the use of (5) and (6) the total radiated power can be calculated, and when normalized with respect to b and λ_0, it is given by the following expression:

$$\frac{P_R\lambda_0}{b}=120\pi\int_0^{\pi/2}|F(\theta)|^2d\theta, \tag{11}$$

where

$$|F(\theta)|=\frac{\sqrt{K_1-\sin^2\theta}\sin\left[\pi\left(\frac{2a}{\lambda_0}\right)\left(\frac{d}{a}-1\right)\cos\theta\right]}{\sqrt{K_1-\sin^2\theta+\cos^2\theta\tan^2\left[\pi\left(\frac{2a}{\lambda_0}\right)\sqrt{K_1-\sin^2\theta}\right]}}+\frac{\cos\theta\tan\left[\pi\left(\frac{2a}{\lambda_0}\right)\sqrt{K_1-\sin^2\theta}\right]\cos\left[\pi\left(\frac{2a}{\lambda_0}\right)\left(\frac{d}{a}-1\right)\cos\theta\right]}{\sqrt{K_1-\sin^2\theta+\cos^2\theta\tan^2\left[\pi\left(\frac{2a}{\lambda_0}\right)\sqrt{K_1-\sin^2\theta}\right]}}. \tag{12}$$

$|F(\theta)|^2$ is the power radiation pattern produced by this configuration. Sample plots of $|F(\theta)|^2$ vs θ for various values of (d/a) and particular values of K_1 and $(2a/\lambda_0)$ are shown in Fig. 3. Since $|F(\theta)|$ is an even function of θ, it is only necessary to plot $F(\theta)$ from 0° to 90°. Graphical techniques have been used on the many sets of curves like those in Fig. 3 to obtain the integral of $|F(\theta)|^2$ and to determine $P_R\lambda_0/b$ as a function of K_1, $(2a/\lambda_0)$, and (d/a). Use was made of (10) and the previously determined properties of the TE_{20} mode in order to calculate $P_z\lambda_0/b$ as a function of K_1, $(2a/\lambda_0)$, and (d/a).

This method of launching the TE_{20} mode is inherently bidirectional, that is, equal amounts of surface wave power will be launched in the positive and negative z-directions. The bidirectional launching efficiency (η) is defined as the ratio of the surface wave power in a desired direction to the total input power.

$$\eta = \frac{P_z}{2P_z + P_R}. \tag{13}$$

It is thus apparent that even if the radiated power could be completely suppressed, the greatest efficiency possible, as defined above, is 50 per cent. A family of curves of the theoretical bidirectional launching efficiency as a function of normalized dielectric slab width $(2a/\lambda_0)$ and normalized current filament position (d/a) is shown in Fig. 4. These curves are for a dielectric constant of 2.56, which is being used in the experimental verification of this theoretical analysis. Similar sets of curves for other dielectric constants have been computed but will not be shown here.

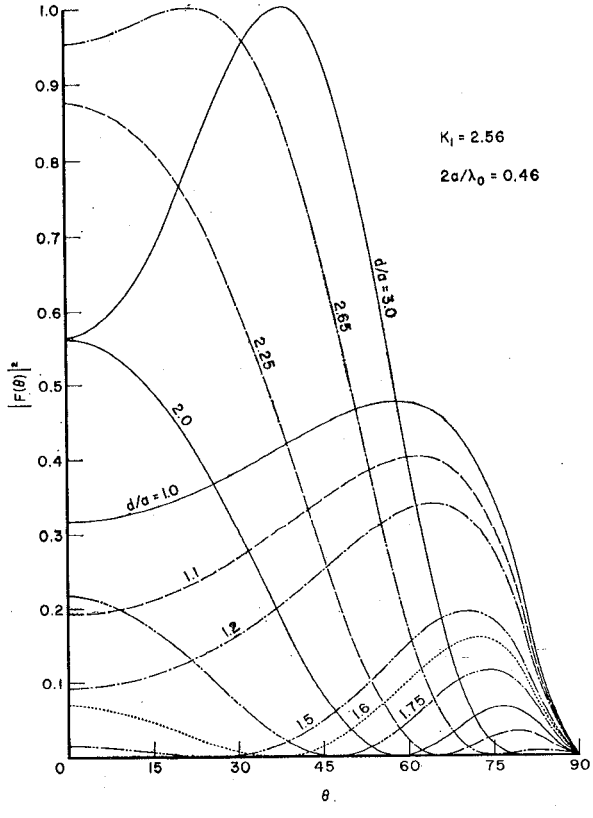

Fig. 3—Power radiation patterns produced by the unit current filament above the dielectric coated conducting plane for various filament locations.

TE_{10} Mode Excitation on a Dielectric Loaded Parallel Plane Waveguide

Whitmer[1] has solved the inhomogeneous wave equation for the case of the infinitesimally thin current filament embedded in the dielectric slab as shown in Fig. 5(a). The solution in this case has restrictions of exponential decay for increasing distance away from the slab in the outer region, but does not have the restriction of the ground plane present in the problem of Tai.[2] The solution found by Whitmer in the region

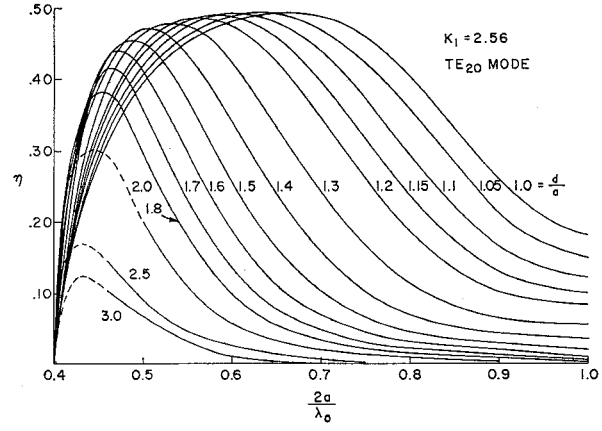

Fig. 4—Bidirectional launching efficiency as a function of dielectric slab width for various values of current filament location.

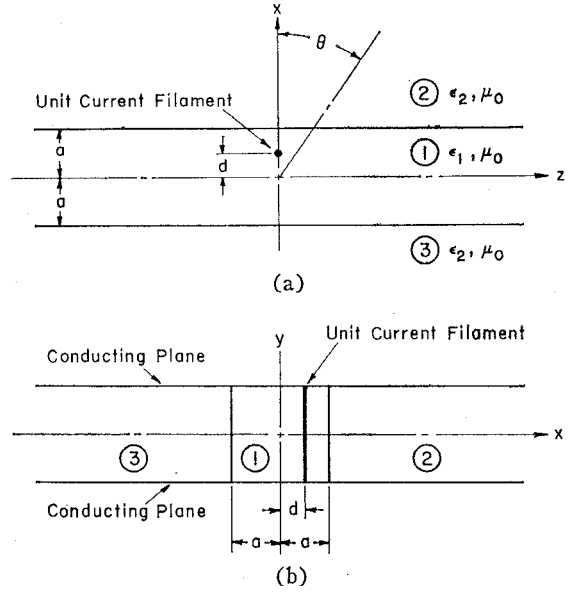

Fig. 5—(a) Infinite dielectric slab excited by an infinitely long unit current filament. (b) Dielectric loaded parallel plane waveguide excited by a unit current filament.

$x>a$, may be written as follows:

$$E_{y2}(x,z) = \frac{j\omega\mu_0}{2\pi}\int_{-\infty}^{\infty} \frac{(k_1+k_2)e^{k_1(a+d)} + (k_1-k_2)e^{-k_1(a+d)}}{(k_1+k_2)^2e^{2k_1a} - (k_1-k_2)^2e^{-2k_1a}} \cdot e^{-k_2(x-a)}e^{j\beta z}d\beta, \tag{14}$$

where k_1 and k_2 are again the x-direction wave numbers of regions 1 and 2 and satisfy (2) and (3). Whitmer has discussed the contributions of poles and branch points in the integrand shown in (14). The same situation exists for this integral as did for the solution of Tai[2], namely, that the poles contribute modal solutions, integration along the branch cut yields the radiation term, and the remainder of the path contributes a vanishing amount in the contour integration.

The integral, (14), has branch points at:

$$\beta_b = \pm\,\omega\sqrt{\mu_0\epsilon_2}, \qquad (k_2 = 0) \tag{15}$$

and poles determined by:

$$(k_{1p}+k_{2p})e^{k_1a} \pm (k_{1p}-k_{2p})e^{-k_1a} = 0. \tag{16}$$

Following a path of integration similar to that shown in Fig. 2 were have found the following contribution for the radiated field after again deforming the path Γ to the path of steepest descents.

$$E_y^R \cong j\sqrt{\frac{\omega\mu_0}{2\pi}}\left(\frac{\mu_0}{\epsilon_0}\right)^{1/4} f(\theta)\,\frac{e^{j\beta_b r}}{r^{1/2}}, \tag{17}$$

where:

$$f(\theta) = \frac{-j[(A-B)e^{jkaA(1+d/a)} + (A+B)e^{-jkaA(1+d/a)}]Be^{-jkaB}}{(A-B)^2e^{j2kaA} - (A+B)^2e^{-j2kaA}},$$

for

$$-\pi/2 \leqq \theta \leqq \pi/2$$

$$f(\theta) = \frac{j[(A+B)e^{jkaA(1-d/a)} + (A-B)e^{-jkaA(1-d/a)}]Be^{jkaB}}{(A+B)^2e^{j2kaA} - (A-B)^2e^{-j2kaA}},$$

for

$$\pi/2 \leq \theta \leq 3\pi/2$$

with

$$A = \sqrt{K_1 - \sin^2\theta}$$
$$B = \cos\theta$$
$$\epsilon_1 = \epsilon_0 K_1, \qquad k = 2\pi/\lambda_0.$$

Whitmer had only indicated this expression with unevaluated constants and for the special case of observation near the slab. Here, we have found asymptotic far field expressions for the radiation in any direction in the space external to the slab, for the purpose of determining the total radiated power.

The interpretation of the pole residue contribution is identical with that discussed in the previous section. In order to satisfy the radiation condition, k_{2p} must again be real and positive and k_{1p} pure imaginary. We let $k_{1p}=jk_{1e}$ and $k_{2p}=k_{2e}$ in order to have pure real transverse wave numbers and to signify the modes of even ("e") symmetry. In the remainder of the analysis of this section, it will be assumed that only the residue of the pole corresponding to the TE_{10} H-guide mode[3] exists. This condition may be assured by proper selection of the slab width according to (8). It has been shown[3] that the TE_{10} mode is the dominant mode of the H-guide when the even symmetry modes are allowed to exist. The even modes may exist, of course, when the center vertical conducting plane (of the trough line) is not present. The TE_{10} mode exists at all frequencies and exists as the sole mode of the H-guide at all frequencies less than the cutoff frequency of the TE_{20} mode.

The condition for the pole becomes:

$$k_{2e} - k_{1e}\tan k_{1e}a = 0. \tag{18}$$

This is identical with that found for the TE_{10} mode[3] and when combined with (2) and (3) yields the conditional equation found previously,[3] for this mode:

$$\pi^2\left(\frac{2a}{\lambda_0}\right)^2(K_1-1) = \left[\frac{k_{1e}a}{\cos k_{1e}a}\right]^2. \tag{19}$$

The solutions of this equation, found graphically,[3] yield the transverse wave number k_{1e} which exists for a given slab width ($2a$) and dielectric constant (K_1).

When the pole residue is evaluated, the following expression for the electric field of the TE_{10} mode in region 2 is found:

$$E_{y2}^s(x,z) = \frac{-\omega\mu_0(k_{1e}a)\cos k_{1e}a\cos k_{1e}d}{2(\beta_p a)(k_{1e}a + \cot k_{1e}a)}e^{-k_{2e}(x-a)+j\beta_p z}. \tag{20}$$

It is again a routine matter to determine the other surface wave field components in both the air and dielectric regions. The normalized total surface wave power may then be calculated:

$$\frac{P_z\lambda_0}{b} = \frac{30\pi^2(k_{1e}a)\cos^2 k_{1e}d}{(k_{1e}a + \cot k_{1e}a)\sqrt{\pi^2\left(\frac{2a}{\lambda_0}\right)^2 - (k_{1e}a)^2}}. \tag{21}$$

The total radiated power in this case is given by:

$$\frac{P_R\lambda_0}{b} = 120\pi\int_0^{\pi} |f(\theta)|^2 d\theta. \tag{22}$$

$|f(\theta)|^2$ is the power radiation pattern of this configuration.

The bidirectional launching efficiency may be calculated by substituting (21) and (22) in (13). Fig. 6 shows the bidirectional launching efficiency computed for polystyrene ($K_1=2.56$) as a function of $2a/\lambda_0$ for various $d/a \leq 1$. Similar curves for other dielectric constants also show that maximum efficiency occurs for $d=0$.

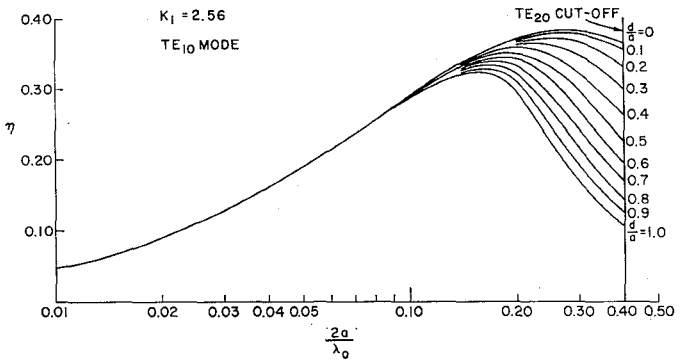

Fig. 6—Bidirectional launching efficiency as a function of dielectric slab width for various values of current filament location.

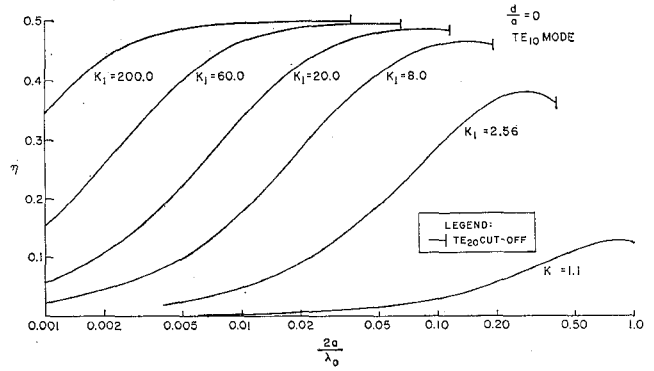

Fig. 7—Bidirectional launching efficiency as a function of dielectric slab width for various values of dielectric constant with center line excitation.

Fig. 7 shows the bidirectional launching efficiency for various dielectric constants vs $2a/\lambda_0$ for $d=0$. Note that the higher dielectric constants have wide ranges of $2a/\lambda_0$ where the efficiency is nearly 50 per cent. This may be verified by arguments of approximate analysis of rays emanating from the current filament. The rays become "trapped" into a mode-like behavior for angles of incidence on the interface greater than or equal to the angle of total internal reflection. Thus, the higher the dielectric constant, the smaller the angle of total reflection and, therefore, the more rays that will be "trapped" into the mode. It should also be noted that as the TE_{10} cutoff ($2a/\lambda_0=0$) is approached, the launching efficiency goes to zero.

Leaky Wave Considerations

In all the discussions above, concerning residue contributions from poles, it has been assumed that the longitudinal and transverse wave numbers had to be either pure real or pure imaginary. The residues from such poles have been defined as "surface waves." Barone[5] has shown that when the complex poles of the propagation constant β are considered, their residues yield "leaky waves." Although difficult to detect, these leaky waves are physically realizable.

The discussion of these contributions is carried out in the transformed complex plane[1,5] $\phi=\xi+i\eta$ (where $\beta=k\sin\phi$), used previously as an aid to the steepest descent integration. In either (1) or (14), the surface wave poles lie along $\xi=\pi/2$, $\eta<0$, and the leaky wave poles lie in the region $0<\xi\leq\pi/2$, $\eta>0$. Residues due to leaky wave poles must be included when the deformation of the path of integration into the steepest descent path causes the pole to be included within the contour integration. As such, the leaky waves merely constitute a portion of the field representation which one has when it is decided to use the saddle point evaluation as a representation of the field. The leaky waves excited by the line source attenuate exponentially along any radius from the origin, for angles within the region of definition.[5] It is therefore apparent that the leaky waves constitute part of the near field of the source in the particular field representation. Furthermore, orthogonality considerations[6] show that the leaky waves are a part of the continuous spectrum of the source, resulting from the evaluation of the field integral along the branch cut described previously. That is, orthogonality is found to exist between each of the surface waves, and between surface waves and the total continuous spectrum, but not between individual terms (saddle point terms and leaky wave terms) of the continuous spectrum.[6]

It then remains to determine if the near fields of the source, including both leaky waves and higher-order contributions of the saddle point evaluation, play any significant role in the experimental measurements described below. Barone[5] has calculated the lower-order waves for the case of our experiment, namely the current source above a grounded slab of polystyrene ($K_1=2.56$). The leaky waves having the lowest rates of attenuation are those for the case of the thickest slab considered.[5] The greatest slab thickness considered in the present work is $2a/\lambda_0=1$, for which thickness, and less, only one leaky wave need be considered.[7] Barone has calculated the rate of attenuation of the leaky wave along the dielectric interface to be about one neper per free space wavelength for a slab thickness of $2a/\lambda_0=1.08$. The initial field strength of the leaky wave in this case has been calculated by the writers to be 19 times that of the surface wave. In seven wavelengths, therefore, the leaky wave will be approximately 35 db below the surface wave field strength at the slab interface. Further calculations of the leaky wave fields and the space wave components, as well as some sample experimental probing of the field within seven wavelengths of the current element in the case $2a/\lambda_0=1.08$, show that the surface wave is certainly dominant in the

[5] S. Barone, "Leaky Wave Contributions to the Field of a Line Source Above a Dielectric Slab," Microwave Res. Inst., Polytechnic Inst. of Brooklyn, N. Y., Rept. 532-56, PIB-462; November, 1956.

[6] L. B. Felsen and N. Marcuvitz, "Modal Analysis and Synthesis of Electromagnetic Fields," Microwave Res. Inst., Polytechnic Inst. of Brooklyn, N. Y., Rept. R726-59; June, 1959.

[7] Wave labeled $N=3$ of Barone, *op. cit.*

vicinity of the slab for distances beyond seven wavelengths.

The absence of effects due to near field distortion should then be obvious in the experiments described below where all measurements of launching efficiency were made with at least seven wavelengths of unobstructed trough line and slab thickness $2a/\lambda_0 \leq 1$.

Launching Efficiency Measurements on the Trough Line TE_{20} Mode

Measurements of the bidirectional launching efficiency as a function of frequency and current filament location have been made on a trough line specified by the following parameters: $K_1 = 2.56$; $a = 3.33$ cm; $b = 0.79$ cm. The method of measuring the launching efficiency is based upon the following scattering matrix analysis of the excitation structure. The trough line and current filament exciter can be considered equivalent to a four-port junction (Fig. 8); port 1 is the coaxial input, ports 2 and 3 are the two surface wave ports, and port 4 is an antenna to account for the radiation loss.

A triple stub coaxial tuner is included between port 1 and the trough line so that a matched input can always be achieved. Matched loads were placed in the trough line on both sides of the current filament and along the top of the trough line in order to provide reflectionless terminations for ports 2, 3, and 4. These loads consisted of tapered sections of white pine wood which were impregnated with a liquid containing suspended carbon. Since the junction is a reciprocal structure, and because of the symmetry between ports 2 and 3, the junction matrix is

$$\begin{vmatrix} b_1 \\ b_2 \\ b_3 \\ b_4 \end{vmatrix} = \begin{vmatrix} s_{11} & s_{12} & s_{12} & s_{14} \\ s_{12} & s_{22} & s_{23} & s_{24} \\ s_{12} & s_{23} & s_{22} & s_{24} \\ s_{14} & s_{24} & s_{24} & s_{44} \end{vmatrix} \cdot \begin{vmatrix} a_1 \\ a_2 \\ a_3 \\ a_4 \end{vmatrix}, \tag{23}$$

where the a's, b's and s's are respectively the elements of the incoming, outgoing, and scattering matrices. The launching efficiency from port 1 to port 3 (η_{13}) is defined as the ratio of the power delivered to a matched load at port 3 to the available power at port 1. With matched loads at ports 2, 3, and 4 ($a_2 = a_3 = a_4 = 0$) and the input matched due to the tuner ($s_{11} = 0$), it is apparent that

$$\eta_{13} = \frac{|b_3|^2}{|a_1|^2} = |s_{12}|^2. \tag{24}$$

If the matched load at port 3 is replaced by a movable short circuit, and if the triple stub tuner is not disturbed (s_{11} is still zero), a standing wave will exist on the coaxial line which feeds port 1. The magnitude of the voltage standing wave ratio will be a function of the position of the short circuit. Positions of the short can be found which will produce a maximum standing wave,

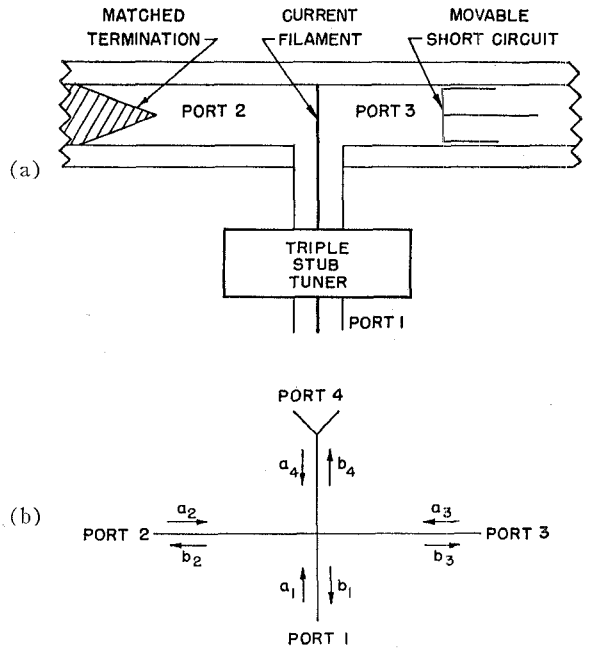

Fig. 8—(a) Top view of trough and current filament exciter. (b) Equivalent four-port junction for current filament exciter.

(VSWR)$_{max}$, or a minimum standing wave, (VSWR)$_{min}$. From (23) it can be shown that

$$\eta_{13} = |s_{12}|^2 = \frac{[(\text{VSWR})_{max} - 1][(\text{VSWR})_{min} - 1]}{(\text{VSWR})_{max} \cdot (\text{VSWR})_{min} - 1}. \tag{25}$$

The accuracy with which the launching efficiency can be measured depends upon how close the reflection coefficient (ρ) of the short is to unity. It can be shown that

$$(\eta_{13})_{measured} = |\rho|\,(\eta_{13})_{true}. \tag{26}$$

Thus, any imperfection of the movable short circuit results in a pessimistic determination of the launching efficiency.

The above method of determining surface wave launching efficiency can be shown to be equivalent to the method of Deschamps[8] for determining the insertion loss of a waveguide junction. Deschamps' method has been used previously[9] to measure launching efficiency.

Launching efficiency was first measured with a short circuit which extended across the air region of the trough line and reached the air-dielectric interface. The resulting measured values of launching efficiency were all much lower than the theoretically predicted values. The short circuit and dielectric slab were modified so that the short extended through the dielectric slab to

[8] G. A. Deschamps, "Determination of reflection coefficients and insertion loss of a waveguide junction," *J. Appl. Phys.*, vol. 24, pp. 1046–1050; August, 1953.

[9] R. H. DuHamel, and J. W. Duncan, "Launching efficiency of wires and slots for a dielectric rod waveguide," IRE Trans. on Microwave Theory and Techniques, vol. MTT-6, pp. 277–284; July, 1958.

nearly the bottom conducting wall of the trough line. Subsequent measurements of bidirectional launching efficiency were made by moving the short circuit and the dielectric slab as an integral unit. These measurements were made over a band of frequencies from 1.8 to 3.6 kmc and for a number of values of normalized current filament location (d/a). Fig. 9 shows a comparison of the measured loss and predicted launching loss for the case where $d/a = 1.11$. The small discrepancy between the measured loss and calculated launching loss is probably due in part to the fact that a perfect short circuit has not yet been achieved.

Measurements were also taken to determine if unidirectional launching efficiencies approaching double those just reported for the bidirectional case could be achieved by properly locating a trough line short circuit on one side of the current filament. These measurements were made by comparing the surface wave power delivered to a matched detector at port 3 with and without a short circuit located at port 2. The power sampled by this detector was measured as a function of frequency. At the center frequency (2.7 kmc), the short was placed at port 2 and adjusted to maximize the power delivered to the detector. The triple stub tuner at the input port was readjusted to provide an input match for this new configuration. After this initial adjustment, the positions of the short and the tuning stubs were held fixed. The increased power delivered to the detector due to the addition of the short and readjustment of the stub tuner was recorded. Thereafter, the frequency was varied across the band and the increase in detected power over that obtained for the bidirectional launching case was measured. The results for this unidirectional launching case are also shown in Fig. 9. This curve shows that the power loss due to this method of launching the TE_{20} mode is extremely low over a broad band of frequencies and that the peak efficiency achieved was 97 per cent.

Conclusions

The bidirectional launching efficiencies of TE surface waves on dielectric loaded trough and parallel plane waveguides excited by a current filament have been derived. Results are shown which indicate the parameters for optimum efficiency. Experimental verification has been carried out in one case.

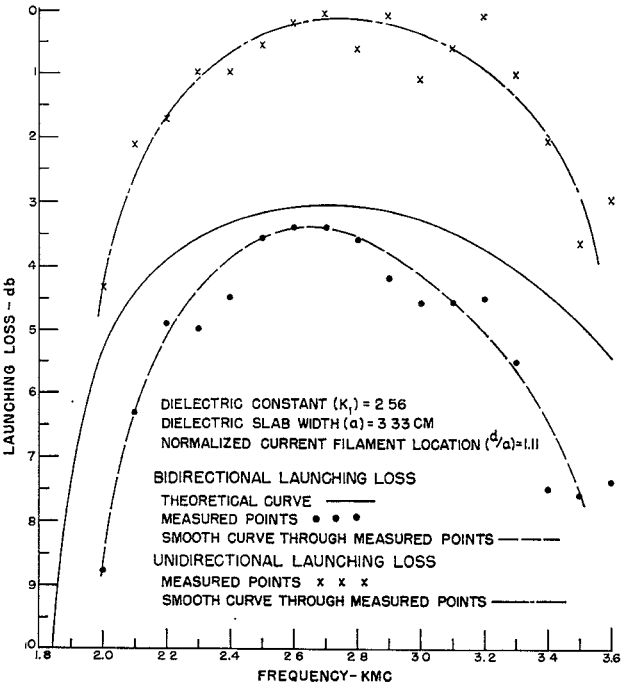

Fig. 9—Curves of unidirectional and bidirectional launching loss for the trough line excited by a current filament.

We conclude not only that is there a method of computing the bidirectional excitation efficiency but also that a unidirectional launching efficiency of 97 per cent can be achieved for this configuration of feed. Finally, these launching techniques are particularly applicable to high dielectric constant lines, where launching is normally difficult.

Acknowledgment

The authors should like to thank Prof. A. A. Oliner and Dr. A. Hessel of the Polytechnic Institute of Brooklyn for reference to the work on leaky waves; Dr. J. M. Kopper for his review of the manuscript; I. E. Pakulis, who performed the measurements; and Miss M. D. Velten for the numerical calculations and curve plotting.